Proc. of the Second Intl. Conf. on Advances In Civil, Structural and Mechanical Engineering- CSM 2014.

978-1-63248-054-5 doi: 10.15224/ 978-1-63248-054-5-97

Ballistic limit of non-filled aluminium tank: Experimental and numerical study

MR. Aziz, W. Kuntjoro, N.V. David

This paper presents the ballistic limit for the non-filled aluminium tank. The main objective was to determine the ballistic limit for the front and rear wall of the tank. In the experiment study, the aluminium tank was 3 mm thick, 150 mm wide and 750 mm long. It was impacted by the fragment simulating projectile (FSP) with the velocity from 239 m/s up to 556 m/s. The numerical models were created with the commercial Altair Hyperworks 12.0. The tank was modeled into two parts, which were the walls impacted by the projectile (front and rear walls) and the lateral wall. The impacted walls had finer element compared with the lateral wall. The impacted walls and lateral wall elements were 0.5 mm^2 and 10 mm^2, respectively. Meanwhile, the FSP was modeled as rigid body. It was observed that the ballistic limit for the front and rear wall tank was 257.7 m/s and 481 m/s, respectively. The numerical study conducted showed the agreement with experimental results.

Keywords— ballistic limit, fragment simulating projectile (FSP), high velocity impact

I. Introduction

The tank failures could lead catastrophic event such as explosion. In 2000, the Concorde had crashed after a few moments took off from the Charles de Gaulle airport (France). The investigation conducted found that the ballistic limit had played a significant role in the incident. Ballistic limit is the minimum velocity required to perforate the target (S. Abrate, 1998). It is also known as V_{50} since the velocity has possibility 50% to perforate and 50% failed to perforate the target.

In the ballistic study, experimental is an important method to employ. In addition, researchers will employ either numerical or analytical study to validate their data. A. Tasdemirci et al (2012), D.W. Zhou and W.J. Stronge (2008), E. Sevkat (2012), N. Kılıc and B. Ekici (2013) and S. Dey et al (2007) employed numerical method as second tool in their works. Meanwhile, researchers such as H.N. Krishna Teja Palleti et al (2012) and Shaktivesh et al (2013) used analytical method as second tool. There are also researchers that employ only experimental data to conduct ballistic limit for instance A. Durmus et al (2011), D. Yunfei et al (2014), E. Wielewski et al (2013), J.B. Jordan and C. J. Naito (2014), Aziz (2013a, 2013b and 2014), N.K. Naik and P. Shrirao (2004), P. Wambua et al (2007) and Z. Tao et al (2012).

There are several targets used by researchers i.e. single metal, double layers metal and composite. A. Durmus et al (2011) conducted study on ballistic limit for cold rolled sheet metals. They found that the projectile flattened and deformed like mushroom at low velocities and separated from the jacket at high velocities. H.N. Krishna Teja Palleti et al (2012) employed experiment and analytical method in their investigation of ballistic limit for the metallic material. They observed that ballistic limit for different thickness can be the same based on the energy absorbing theory. Z. Tao et al (2012) employed Titanium Alloy as target in their works. They proposed an empirical equation that can predict the ballistic limit. MR Aziz et al (2013a and 2013b) carried out experiment to determine the ballistic limit for the non-filled aluminium tank In the following year, 2014, MR Aziz et al detailed further the ballistic limit by determining the terminal ballistic. They stated that there were four main stages which were the first contact between projectile and the tank, partial perforation, full perforation with projectile and plug still intact and lastly separation of projectile and plug. N. Kılıc and B. Ekici (2013) studied the ballistic limit for armor steels by employing experiment and numerical method. Good agreement was observed between these two methods.

S. Dey et al (2007) analyzed the ballistic limit for the double layers of steel plates. They suggested that the lowest ballistic limit increased drastically when the target had double layers. D.W. Zhou and W.J. Stronge (2008) conducted ballistic limit for two layers steel sheets. They found that the ballistic limit was influenced by space between layers. E. Wielewski et al (2013) employed multi-layer plate, which was fibre reinforced plastic as the target. They observed that the resistance of ballistic perforation was affected by the ratio of plies between layers. D. Yunfei et al (2014) investigated ballistic performance of double-layered steel plates. They stated that the ballistic limit was higher when upper layer had high strength with low ductility and lower layer had low strength and high ductility employed.

N.K. Naik and P. Shrirao (2004) carried out an experiment on ballistic impact of woven fabric composites. Among result obtained was different type of failures, which were cone formation, tensile failure, deformation of secondary yarns, delamination, matrix cracking, shear plugging and friction

MR. Aziz
Universiti Teknologi MARA (UiTM)
Malaysia

W. Kuntjoro
Universiti Teknologi MARA (UiTM)
Malaysia

N.V.David
Universiti Teknologi MARA (UiTM)
Malaysia

Proc. of the Second Intl. Conf. on Advances In Civil, Structural and Mechanical Engineering- CSM 2014.

978-1-63248-054-5 doi: 10.15224/ 978-1-63248-054-5-97

during penetration. P. Wambua et al (2007) studied the ballistic response of natural fibre. The results showed that the composites failed by shear cut-out, delamination and fibre fracture. A. Tasdemirci et al (2012) analyzed ballistic limit for ceramic/composite armors. Through their experiment and numerical study, they suggested that Teflon and aluminium foam interlayer could lead to the delay and also reduction of the stress transmitted to the composite. E. Sevkat (2012) conducted experiment and numerical study on ballistic limit velocities of woven composite beams. They proposed nonlinear-orthotropic material model which able to simulate the ballistic response. Shaktivesh et al (2013) investigated ballistic limit for the polymer matrix. They claimed that their analytical approach successfully predicted the ballistic limit and plug dimension. J.B. Jordan and C.J. Naito (2014) carried out study by employed E-Glass/Phenolic glass fiber reinforced plastic (GFRP) as target. They concluded that the ballistic response and energy absorbed was affected by the nose shape of the projectile.

From the literature reviews above, it is clearly shown that there is a need to conduct ballistic limit for the empty aluminium tank for both experiment and numerical methods. MR Aziz et al (2013a, 2013b and 2014) in their works concentrated in the experiment only. Therefore this paper intends to contribute to the pool of knowledge by adding the numerical method approach to the problem.

II. Methodology

A. *Experimental setup*

The aluminium tank was 3 mm thick, 150 mm wide and 750 mm long. It was closed with two Polymethyl methacrylate (PMMA) windows, which fixed to the four steel bars. The contact points between PMMA windows and the tank was sealed with silicone to prevent any leakage. Figure 1 shows the actual and schematic diagram of the aluminium tank.

The tank was impacted with fragment simulating projectile (FSP). It was cylindrical with a blunt chisel shaped nose and a raised flange at the base. It was fixed into the 7.62 mm jacket with sabot. The FSP had 1.1 g of weight, which was launched by gas gun. In order to vary the velocities, different weight of charge was put into the bullet's jacket. The velocity varied from 239 m/s to 972 m/s. Figure 2 shows the completed projectile, sabot and FSP. ProChrono Digital Chronograph was employed to capture the velocity of the FSP. For better lighting, one Hydrargyrum medium-arc iodide (HMI) lamp with 1200 Watt was located at the test area. Figure 3(a) until 3(c) show the actual equipment employed in the experiment.

Figure 1: Actual and schematic diagram of the tank

Figure 2: Completed projectile (left), sabot (middle) and FSP (right)

3(a): ProChrono Digital Chronograph

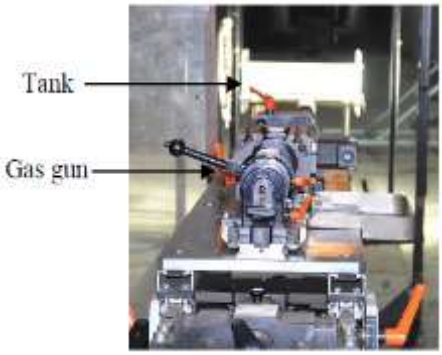

3(b): Gas gun and tank

3(c): Hydrargyrum medium-arc iodide (HMI) lamp

Figure 3: Equipment of the test

Proc. of the Second Intl. Conf. on Advances In Civil, Structural and Mechanical Engineering- CSM 2014.

978-1-63248-054-5 doi: 10.15224/ 978-1-63248-054-5-97

B. *Numerical simulation*

The numerical models were created with the commercial Altair Hyperworks 12.0. It has the capability of modeling, analysis, visualization solutions for linear, non-linear, structural optimization, fluid-structure interaction, and multi-body dynamics applications. For modeling purpose, HyperMesh was employed. It is a high-performance finite-element pre-processor that provides a highly interactive and visual environment. Then, for the processing, RADIOSS was employed. RADIOSS is a leading structural analysis solver for highly non-linear problems under dynamic loadings. The results were visualized by using HyperView. It is a complete post-processing and visualization.

The tank was modeled into two parts, which were the walls impacted by the projectile (front and rear walls) and the lateral wall. The impacted walls had finer element compared with the lateral wall. The impacted walls and lateral wall elements were 0.5 mm^2 and 10 mm^2, respectively as shown in Figure 4. Meanwhile, the FSP was modeled as rigid body. For the tank, the Johnson-Cook failure model was employed. It was suitable for the isotropic elastic-plastic material. The stress-strain relation is given by following equation:

$$\sigma = (a + b\varepsilon_p^n)(1 + c.ln\frac{\dot{\varepsilon}}{\dot{\varepsilon_0}})(1 - T^{*m}) \quad (1)$$

where σ is the stress level, ε_p^n is the plastic strain, a is the yield stress, b is the hardening modulus, n is the hardening exponent, c is the strain rate coefficient, $\dot{\varepsilon}$ is the strain rate and $\dot{\varepsilon_0}$ is the reference strain rate. The first bracket on the right hand side of the equation represents the influence of plastic strain. The second bracket and third bracket represents the influence of strain rate and the influence of temperature change, respectively. Table 1 shows the material properties for the tank and projectile. These parameters were obtained from MR Aziz et al (2014) works.

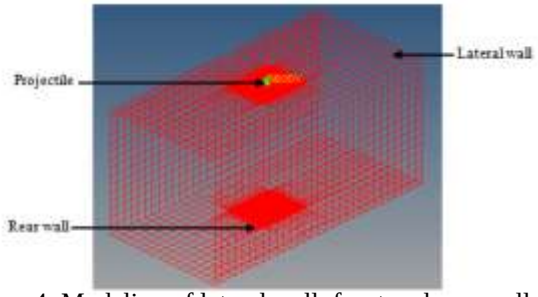

Figure 4: Modeling of lateral wall, front and rear wall and projectile

TABLE 1: MATERIAL PROPERTIES

Material	ρ	E	υ	a	b	n
Aluminium 195-T6	2770 kg/m^3	72.6 GPa	0.35	160 MPa	127 MPa	0.51
Steel 4340H	7861 kg/m^3	205 GPa	0.29	-	-	-

III. Results and Discussion

A. *Ballistic limit*

The ballistic limit was calculated by taking the average of an equal number of highest partial perforation and the lowest perforation velocities. Table 2 shows the FSP's velocities and the result obtained when the projectile impacted the front wall. When the FSP was launched with the velocities of 239 m/s, 248 m/s and 253 m/s, the FSP failed to perforate the front wall successfully. But, when the velocity was increased to 265 m/s, the FSP successfully perforated the front wall. Same results were observed when the FSP launched with 268 m/s and 273 m/s. By average, the ballistic limit for front wall was equal to 257.7 m/s. The numerical simulation showed slightly different result, which 260 m/s.

TABLE 2: FRONT WALL TEST

Velocity (m/s)	Result
239	Partial perforated
248	Partial perforated
253	Partial perforated
265	Perforated
268	Perforated
273	Perforated

Meanwhile for the rear wall, the velocity of the FSP impacted the wall was determined using equation by Brenda et al (2010):

$$V_R = A(V_0^p - V_{BL}^p)^{1/p} \quad (2)$$

V_R is the residual velocity, A and p are the empirical parameters, V_0 is the impact velocity and V_{BL} is the ballistic limit velocity of the front wall. Therefore, the residual velocity can be determined which represented the velocity that impacted the rear wall. The chronograph employed in this study was able to capture the velocity that impacted the front wall only. Table 3 summarized the FSP's velocities, the residual velocities and the result of the perforation. When the residual velocities i.e. velocities that impacted the rear wall were 460.8 m/s, 463.1 m/s and 488.2 m/s, the FSP failed to perforate the rear wall successfully. As the residual velocities became 489.3 m/s, 491.5 m/s and 492.7 m/s, the FSP able to perforate the rear wall. So, in this case, the ballistic limit for the rear wall was 481 m/s. Meanwhile, the ballistic limit obtained from the numerical simulation was 497 m/s.

TABLE 3: REAR WALL TEST

Velocity (m/s)	Residual velocity (m/s)	Result
528	460.8	Partial perforated
530	463.1	Partial perforated
552	488.2	Partial perforated
553	489.3	Perforated
555	491.5	Perforated
556	492.7	Perforated

Proc. of the Second Intl. Conf. on Advances In Civil, Structural and Mechanical Engineering- CSM 2014.

978-1-63248-054-5 doi: 10.15224/ 978-1-63248-054-5-97

B. *Modes of failure*

H.N. Krishna Teja Palleti et al (2012) stated in their works that the ballistic test involved plastic perforation, bulge formation, bulge advancement, plug formation and the exit of the projectile. From the study conducted, the bulge formation happened when the FSP partially perforated the wall. Then after the bulge advancement, the FSP perforated the wall successfully. Figure 5(a) and 5(b) show the pictures of the partial perforation of the FSP for both experiment and numerical simulation. There were two types observed i.e. straight and slant. It was believed that it was due to the velocity that impacted the wall. If the velocity was high to travel after the firing, the FSP went straight to the wall with high momentum. Unfortunately, the FSP did not has enough momentum to perforate the tank fully. But if the velocity was quite low to travel after the firing, the FSP embedded in the slant direction. Both failures happened at the front and rear wall of the tank.

When the FSP perforated the wall fully, the main failure combined plugging and petalling (Z. Tao et al, 2012). Figure 6(a) to 6(c) show the deformation of the wall for this case for both results from the experiment and numerical simulation. Figure 6(a) and 6(b) show the result from the top view and Figure 6(c) shows the result from the side view. It can be seen clearly the petalling failure mode occurred.

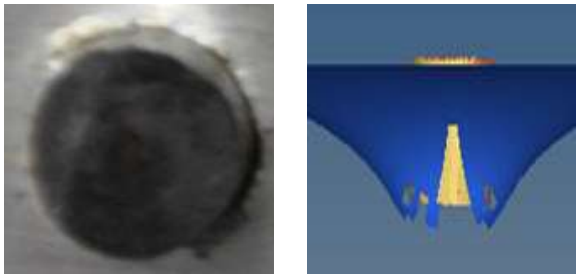

(a) Straight

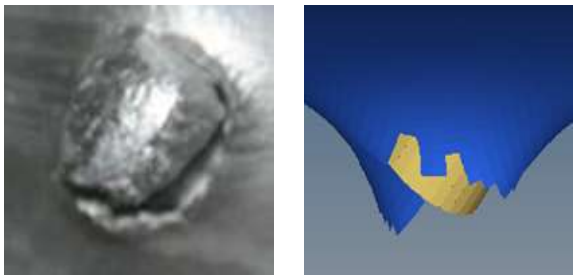

(b) Slant

Figure 5: Partial perforation

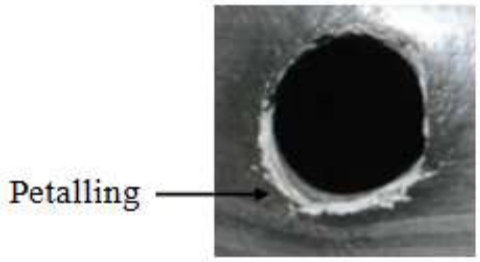

6(a) Top view (experiment)

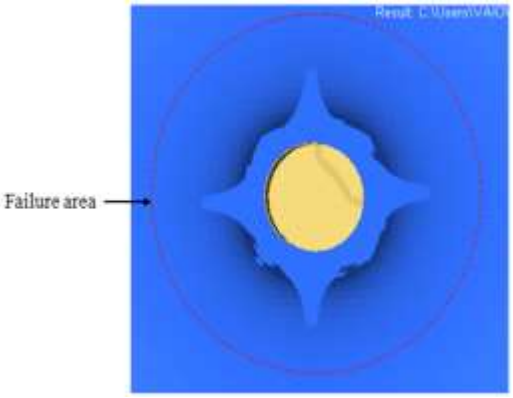

6(b) Top view (numerical simulation)

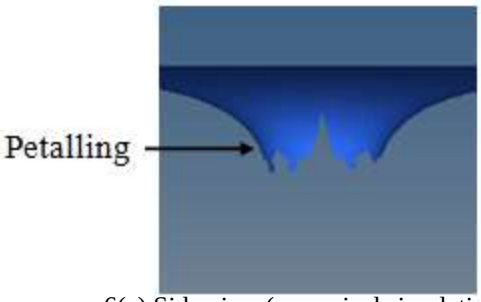

6(c) Side view (numerical simulation)

Figure 6: Full perforation

C. *Stages of failures*

There were five main stages for the fully perforation case. The first one was the contact between the FSP and the wall of the tank as shown in the Figure 7(a). Then, the partial perforation of the FSP, followed by the fully perforation. Figure 7(b) and 7(c) shows these two failures, respectively. Next, in the Figure 7(d), the FSP travelled in the tank. At this time, there were two types of modes were observed i.e. the FSP travelled with straight direction or with slant direction. Commonly, the slant direction occurred when the FSP was about to make a kink the second wall rather than to perforate it. Last stage occurred when the FSP exit the tank.

Proc. of the Second Intl. Conf. on Advances In Civil, Structural and Mechanical Engineering- CSM 2014.

978-1-63248-054-5 doi: 10.15224/ 978-1-63248-054-5-97

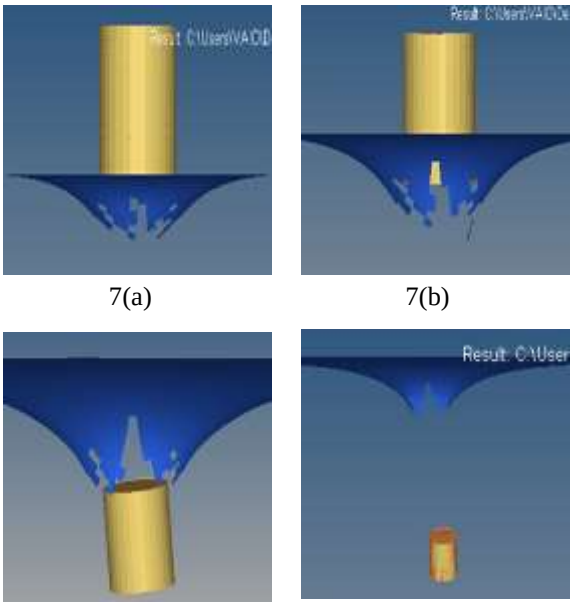

7(a) 7(b)

7(c) 7(d)

Figure 7: Stages of failures

IV. Conclusion

The ballistic limit study for the non-filled aluminum tank has been successfully conducted. Generally, good agreement between experiment and numerical simulation was achieved. The ballistic limit for the front and rear wall was 257.7 m/s and 481 m/s, respectively. Result obtained from simulation showed slightly different, 260 m/s for the front wall and 497 m/s for the rear wall. Two main failures modes observed i.e. partial perforation and full perforation. Meanwhile there were five stages of the failures, namely first contact, partial perforation, full perforation, travelling period and exit phase.

Acknowledgment

The authors would like to thanks Ministry of Science, Technology and Innovation (MOSTI) Malaysia for the financial support through e-Science Fund 06-01-01-SF0509 and Research Management Institute (RMI) UiTM.

References

[1] A. Durmu, M. Güden, B. Gülçimen, S. Ülkü, E. Musa., "Experimental investigations on the ballistic impact performances of cold rolled sheet metals", Materials and Design, 32, pp. 1356–1366, 2011.

[2] A. Tasdemirci, G. Tunusoglu, M. Güden., "The effect of the interlayer on the ballistic performance of ceramic/composite armors: Experimental and numerical study", International Journal of Impact Engineering, 44, pp. 1-9, 2012.

[3] Brenda L. Buitrago, Shirley K. García-Castillo, Enrique Barbero, "Experimental analysis of perforation of glass/polyester structures subjected to high-velocity impact," Materials Letters, 64, pp. 1052–1054, 2010.

[4] Deng Yunfei, Zhang Wei, Yang Yonggang, Shi Lizhong, Wei gang., "Experimental investigation on the ballistic performance of double layered plates subjected to impact by projectile of high strength", International Journal of Impact Engineering, 70, pp. 38-49, 2014.

[5] D.W. Zhou, W.J. Stronge, "Ballistic limit for oblique impact of thin sandwich panels and spaced plates", International Journal of Impact Engineering, 35, pp. 1339–1354, 2008.

[6] Euan Wielewski, Alan Birkbeck, Ron Thomson., "Ballistic resistance of spaced multi-layer plate structures: Experiments on Fibre Reinforced Plastic targets and an analytical framework for calculating the ballistic limit", Materials and Design, 50, pp. 737–741, 2013.

[7] Ercan Sevkat., "Experimental and numerical approaches for estimating ballistic limit velocities of woven composite beams", International Journal of Impact Engineering, 45, pp. 16-27, 2012.

[8] H.N. Krishna Teja Palleti, S. Gurusamy, Santosh Kumar, R. Soni, B. John, R. Vaidya, A. Bhoge, N.K. Naik., "Ballistic impact performance of metallic targets", Materials and Design, 39, pp. 253–263, 2012.

[9] Joseph B. Jordan , Clay J. Naito, "An experimental investigation of the effect of nose shape on fragments penetrating GFRP", International Journal of Impact Engineering, 63, pp. 63-71, 2014.

[10] MR. Aziz, W. Kuntjoro, NV. David, F. Rais, "An Experimental Study on the Ballistic Impact Behavior of Non-filled Tank against Fragment Simulating Projectile (FSP)", Applied Mechanics and Materials, Trans Tech Publications, Vol. 393, pp 409-414, 2013.

[11] MR. Aziz, W. Kuntjoro, NV. David, R. Ahmad., "Ballistic Resistance Analysis of Non-filled Tank against Fragment Simulating Projectile (FSP)", Journal of Mechanical Engineering, 10(2), pp. 79-95, 2013.

[12] MR. Aziz, W. Kuntjoro, NV. David., "Terminal Ballistic Experimental Analysis of An Empty and Full Water Tank", a Chapter in the WIT Transactions on Built Environment, 141, pp. 191 – 203, 2014.

[13] N.K. Naik, P. Shrirao, "Composite structures under ballistic impact Composite structures under ballistic impact", Composite Structures, 66, pp. 579–590, 2004.

[14] Namık Kılıç, Bülent Ekici., "Ballistic resistance of high hardness armor steels against 7.62 mm armor piercing ammunition", Materials and Design, 44, pp. 35–48, 2013.

[15] Paul Wambua, Bart Vangrimde, Stepan Lomov, Ignaas Verpoest, "The response of natural fibre composites to ballistic impact by fragment simulating projectiles", Composite Structures, 77, pp. 232–240, 2007.

[16] S. Abrate, Ballistic impact, Impact on Composite Structure, (Cambridge University Press, 1998), pp 215-224.

[17] S. Dey, T. Børvik, X. Teng, T. Wierzbicki, O.S. Hopperstad., "On the ballistic resistance of double-layered steel plates: An experimental and numerical investigation", International Journal of Solids and Structures, 44, pp. 6701–6723, 2007.

[18] Shaktivesh, N.S. Nair, Ch.V. Sesha Kumar, N.K. Naik., "Ballistic impact performance of composite targets", Materials and Design, 51, pp. 833–846, 2013.

[19] ZHANG Tao, CHEN Wei, GUAN Yupu, GAO Deping., "Study on Titanium Alloy TC4 Ballistic Penetration Resistance Part I: Ballistic Impact Tests", Chinese Journal of Aeronautics, 25, pp. 388-395, 2012.

About Author (s):

MR. Aziz is currently doing his Ph.D in Impact Mechanics at Universiti Teknologi MARA, Malaysia. He obtained his bachelor degree and master in Mechanical Engineering from Universiti Sains Malaysia, Malaysia.

W. Kuntjoro is a professor at the Faculty of Mechanical Engineering, Universiti Teknologi MARA, Malaysia. He teaches and researches in the area of Lightweight Structures, Aircraft Design, and Structural Integrity.

NV. David is a lecturer at Faculty of Mechanical Engineering at Universiti Teknologi MARA, Malaysia. He obtained his PhD from Dwight Look College of Engineering,Texas A&M University, College Station, Texas, USA in Sound & Vibration.